STEM CELLS AND DEVELOPMENT
Volume 24, Number 23, 2015

DOI: 10.1089/scd.2015.0107

Autologous Bone Marrow Mononuclear Cells Exert Broad Effects on Short- and Long-Term Biological and Functional Outcomes in Rodents with Intracerebral Hemorrhage

Satoshi Suda,[1,*] Bing Yang,[2,*] Krystal Schaar,[2] Xiaopei Xi,[2] Jennifer Pido,[2] Kaushik Parsha,[2] Jaroslaw Aronowski,[2] and Sean I. Savitz[2]

Autologous bone marrow-derived mononuclear cells (MNCs) are a potential therapy for ischemic stroke. However, the effect of MNCs in intracerebral hemorrhage (ICH) has not been fully studied. In this study, we investigated the effects of autologous MNCs in experimental ICH. ICH was induced by infusion of autologous blood into the left striatum in young and aged male Long Evans rats. Twenty-four hours after ICH, rats were randomized to receive an intravenous administration of autologous MNCs (1×10^7 cells/kg) or saline. We examined brain water content, various markers related to the integrity of the neurovascular unit and inflammation, neurological deficit, neuroregeneration, and brain atrophy. We found that MNC-treated young rats showed a reduction in the neurotrophil infiltration, the number of inducible nitric oxide synthase-positive cells, and the expression of inflammatory-related signalings such as the high-mobility group protein box-1, S100 calcium binding protein B, matrix metalloproteinase-9, and aquaporin 4. Ultimately, MNCs reduced brain edema in the perihematomal area compared with saline-treated animals at 3 days after ICH. Moreover, MNCs increased vessel density and migration of doublecortin-positive cells, improved motor functional recovery, spatial learning, and memory impairment, and reduced brain atrophy compared with saline-treated animals at 28 days after ICH. We also found that MNCs reduced brain edema and brain atrophy and improved spatial learning and memory in aged rats after ICH. We conclude that autologous MNCs can be safely harvested and intravenously reinfused in rodent ICH and may improve long-term structural and functional recovery after ICH. The results of this study may be applicable when considering future clinical trials testing MNCs for ICH.

Introduction

Spontaneous intracerebral hemorrhage (ICH) is one of the most lethal forms of stroke that accounts for 10% of all strokes, resulting in 30%–50% mortality by 1 month; most survivors remain disabled [1,2]. Although therapies for acute ischemic stroke such as thrombolysis and mechanical clot removal have been developed, there is no effective medical therapy for patients with ICH. Treatment is limited to supportive care or invasive neurosurgical evacuation of the hematoma in selective patients [3].

Cell-based therapy is actively being investigated as a new potential treatment for neurological disorders, including stroke. Various types of cells, including neural stem cells, embryonic stem cells, mesenchymal stem cells, and adipose stem cells, have been found to improve neurological outcome in animal stroke models [4–7]. Bone marrow-derived mononuclear cells (MNCs) are composed of diverse cell populations and are attractive as a cell therapy for the acute stage of stroke because they permit rapid bone marrow harvest and separation for autologous transplantation [8]. Previous studies have shown that MNCs enhance recovery in rodent models of ischemic stroke. Since other types of cell therapy such as human neural stem cells or allogenic marrow stromal cells have protective effects in the ICH model [9–11], we aimed to determine whether autologous MNCs can ameliorate brain injury after ICH.

In the present study, we investigated whether autologous MNC delivery at 24 h after ICH in a clinically relevant manner could attenuate inflammation and brain edema and improve long-term motor and cognitive function after experimental ICH. We assessed potential mechanisms of the protective effects of MNCs.

[1]Department of Neurological Science, Graduate School of Medicine, Nippon Medical School, Tokyo, Japan.
[2]Department of Neurology, University of Texas Medical School at Houston, Houston, Texas.
*These authors contributed equally to this work.

Materials and Methods

Animals

In this study, 110 young male Long Evans rats weighing 275–325 g were involved in all experiments and 71 aged male Long Evans retired breeder rats weighing 600–650 g were used in selective experiments. All animal experiments and surgical procedures were approved by the University of Texas Health Science Center Animal Welfare Committee and followed National Institutes of Health guidelines and regulations.

Intracerebral hemorrhage model

Animals were anesthetized with isoflurane (2.0%) in 70% O_2/30% N_2O through spontaneous respiration, and core temperature was maintained at 37°C ± 0.5°C throughout all surgical procedures with the use of a heating pad. Primary ICH was induced by direct infusion of autologous blood into the striatum [12,13]. Briefly, a midline scalp incision was made, and a hole was drilled in the left side of the skull (from bregma: 0.5 mm posterior, 4.5 mm lateral). Fresh (nonheparinized) autologous whole blood was collected from the tail artery. A 26-gauge needle attached to the syringe was inserted stereotaxically into the left striatum (with 5.75 or 6.25 mm depth). The blood (70 μL) was infused at a rate of 10 μL/min, and the needle was left in place for another 20 min to minimize backflow. The needle was then withdrawn very slowly. The hole in the skull was sealed with bone wax, and the scalp was sutured. After the surgery, the animals were placed in a clean cage and allowed free access to water and food at ambient temperature. In the sham group, rats underwent the same surgical procedures as in the ICH group, including the needle insertion into the striatum but without blood infusion.

Bone marrow harvest

Bone marrow harvest was performed 22 h after ICH, as previously described [14]. Animals were anesthetized with isoflurane 2% in 70% O_2/30% N_2O. An incision was made through the skin to the medial aspect of the tibia of the unimpaired limb. The periosteum was removed, and the surgeon drilled a burr hole extending into the medullary cavity. A 20-gauge hypodermic needle was inserted into the medullary cavity and connected to a heparinized syringe. Bone marrow (1–1.5 mL) was aspirated while rotating and moving the needle back and forth. In the saline control group, the same procedure was performed involving a burr hole and needle insertion of the tibia without bone marrow aspiration. The burr hole was sealed with bone wax, the skin was closed with a nylon suture, and 0.25% Marcain was given locally. In the sham and saline control groups, rats underwent the same surgical procedures but without the aspiration of bone marrow. This limited aspiration of the bone marrow does not cause impairment of the limbs, and animals are able to participate fully in neurological testing [14].

MNC isolation and administration

As described previously [15], the cells from the bone marrow aspirate were triturated, centrifuged, and washed in phosphate-buffered saline (PBS) +0.5% bovine serum albumin (BSA). Cells were then suspended in medium 199 and counted using a hemocytometer and Coulter counter. The cell suspension was added on top of 20 mL Ficoll-Paque Plus in a 50-mL conical vial and then centrifuged. The MNCs were collected, washed with PBS +0.5% BSA, and then counted. MNC viability was more than 98% by trypan blue detection. MNCs were then suspended in 1 mL sterile cold PBS. The overall procedure took 2 h to complete. We previously reported the immunophenotypes of MNCs from Long Evans rats using this procedure [15]. For intravenous delivery, the tail vein was isolated under a surgical microscope. One milliliter of MNCs (1×10^7 cells/kg) or saline was infused over 5 min 24 h after ICH. We chose this dosage based on our previous preclinical and clinical studies on ischemic stroke [8,16].

Immunophenotypes of MNCs

Since MNCs are a heterogenous population from our previous studies [14,15], we investigated the subpopulations within the MNCs. Rats was subjected to ICH ($n = 5$). At 22 h after injury, bone marrow was aspirated and MNCs were isolated. We performed flow cytometry to characterize the MNC population using a previously published protocol. Briefly, 1×106 MNCs were suspended in a 100 μL staining buffer (Hank's Balanced Salt Solution + 2% FBS), then were incubated with anti-rat antibodies specific for CD3-FITC, CD45-FITC, CD90-PE, CD29-APC (1:100; BioLegend); CD11b-FITC, CD45R-PE, CD71-PE, CD161a-PE (1:100; BD Bioscience); CD34-PE (1:5; Santa Cruz Biotechnology). The mice IgG isotypes for PE, FITC, and APC per antibody were tested as controls, respectively. Stained cell were collected using Gallios Flow Cytometer (Beckman Coulter) and analyzed with Kaluza software (Beckman Coulter).

Fluoro-J staining

To detect whether MNCs were able to reduce neuronal cell death induced by ICH, we quantified dead neurons in the perihemotomal area with Fluoro-J staining. Briefly, rats were perfused intracardially with ice-cold PBS at day 3 after MNC or saline infusion in the ICH model as described above. Fresh frozen sections were selected from the perihematomal tissue of the brain at the level of +1 to −1 mm relative to the needle insertion point. Forty micrometer thick slices were generated and fixed with cold 2% paraformaldehyde (PFA) (for 20 min), followed by a staining protocol we reported previously [17]. Four views were randomly selected from the perihemotomal region in each cryosection, and neuronal death was visualized and analyzed for the abundance of fluorescent cells under a fluorescence microscope.

Serum cytokine measurements

To examine the impact of MNCs on the systemic inflammatory response after ICH, we collected blood samples pre-ICH, day 1 after ICH but pre-MNC treatment, and day 3 after ICH. Interleukin (IL)-1β and IL-10 (Thermo Scientific) were detected by an enzyme-linked immunosorbent assay according to the manufacturers' protocols.

Immunohistochemistry slice

At 3 or 28 days after ICH, rats were perfused intracardially with ice-cold PBS. Brains were then harvested and

snap-frozen. In the cryostat, brains were divided into six coronal pieces (2 mm, I–VI). Three coronal 10 μm cryosections from section III–V were selected and cut onto slides and then fixed by 2% PFA for 30 min at room temperature or treated with acetone for 30 min at −20°C, respectively. After blocking for 2 h in 5% goat serum and 0.01% Triton X-100 in PBS at room temperature, the cryosections were incubated with primary antibodies: rabbit polyclonal anti-rat myeloperoxidase (MPO; to visualize neutrophils) (1:500; Dako), mouse monoclonal anti-rat OX-42 (to visualize microglia) (1:100; Abcam), and rabbit polyclonal anti-rat inducible nitric oxide synthase (iNOS) (1:100; Abcam) for day 3 assay after ICH; mice monoclonal anti-rat CD31 antibody (1:100; MAB) (to visualize endothelium) and rabbit polyclonal anti-rat doublecortin (DCX) antibody (1:1,000; Abcam) (to visualize neuronal precursor cells, cryosection only from brain section IV) for day 28 assay after ICH. Then, secondary antibodies conjugated to Alexa Fluor 488 or Alexa Fluor 568 (1:800; Invitrogen) for 2 h at room temperature. The immunofluorescence signal was captured under the view with 200× magnification using fluorescence microscope equipped with charge-coupled device camera, and all immunopositive cells were counted using ImageJ software (NIH) as described previously [17]. For DCX-positive cell analysis, three views were randomly selected from the subventricular zone in each cryosection. For other positive cells or CD31-positive vessel analysis, four views were randomly selected from the perihemotoma region in each cryosection.

Western blot analysis

At 3 days after ICH, rats were perfused intracardially with ice-cold PBS. Brains were harvested. The injured ipsilateral hemisphere was homogenized on ice in a radioimmunoprecipitation assay buffer (Invitrogen). The protein concentration of each sample was determined using the Bicinchoninic Acid Assay (Sigma-Aldrich). Fifty micrograms of protein was separated on a 4%–12% gradient sodium dodecyl sulfate–polyacrylamide gel electrophoresis (SDS-PAGE) gel using a Novex Mini Cell system (Invitrogen). The proteins were transferred onto a polyvinylidene fluoride membrane (Invitrogen) using the Novex Mini Cell system. Membranes were blocked (5% nonfat milk, 0.1% TWEEN-20 in Tris-buffered saline, pH 7.6) at room temperature for 2 h and incubated with primary antibodies overnight at 4°C. We used 1:1,000 rabbit monoclonal anti-rat S100 calcium binding protein B (S100β; Abcam), 1:1,000 rabbit polyclonal anti-rat matrix metalloproteinase 9 (MMP9; Abcam), 1:1,000 rabbit polyclonal anti-rat high-mobility group protein box-1 (HMGB1; Santa Cruz Biotechnology), and 1:1,000 rabbit polyclonal anti-rat aquaporin 4 (AQP4; Abcam) as primary antibodies. Mouse monoclonal anti-rat β-actin (1:2,000; Sigma-Aldrich) was used as a normalizing control. Horseradish peroxidase-conjugated mouse monoclonal antibodies (eBioscience, USA) to rabbit and goat were used as secondary antibodies, respectively, and membranes were incubated for 1 h at room temperature. Immunoreactive bands were visualized using an enhanced chemiluminescence system (GE Healthcare) according to the manufacturer's protocol. X-ray films were scanned and then analyzed with ImageJ for densitometric analyses.

Morphometric measurement of hemispheric atrophy

At day 28 after ICH, rats were euthanized to analyze hemispheric atrophy. Animals were anesthetized and intracardially perfused with ice-cold PBS and decapitated. Brains were harvested and divided into six sections (2 mm, I–VI). Five coronal 20 μm frozen sections from section II to VI were stained with cresyl violet. The hemispheric areas of each slide from each section were traced and measured using ImageJ software (NIH). The hemispheric atrophy was expressed as a percentage of contralateral hemispheric area [18].

Measurement of brain water content

At day 3 after ICH, animals were overdosed with isoflurane and decapitated and their brains were removed immediately. The cerebellum and brain stem were excised. The remaining forebrain was divided along the midline, and wet weights were measured. Dry weights were obtained after drying for 48 h in an oven at 80°C. Water content was expressed as a percentage of the wet weight: the formula for calculation was (wet weight − dry weight)/(wet weight) × 100 [18,19].

Motor test

Young animals underwent long-term behavioral testing that was performed by an examiner blinded to treatment allocation. Animals were pretested before ICH and then tested on days 7, 14, 21, and 28 after ICH. The staircase test was used to evaluate limb dysfunction in our model. The staircase test is an efficient test that assesses reaching capacity, dexterity, and motor coordination of the impaired forelimb [20]. It evaluates independent forelimb function [21] and has been reported to be more sensitive to detecting long-lasting deficits in the ICH model compared with other behavior tests [22–24]. As described previously [20], our apparatus consisted of seven steps on each side. Three pellets were placed in each well for a total of 21 pellets on each side. Testing trials consisted of 10 min sessions. At the end of each testing trial, the total number of pellets collected on the impaired side was recorded. In addition, the lowest step (numbered 1–7, starting from the top) reached was that from which at least one pellet had been displaced. All animals were pretrained for 3 weeks, and baseline values were recorded before surgery.

Water maze test

To avoid potential interference of demanding training required for the staircase test, we used separate groups of animals in the Morris water maze to assess cognitive function. Both young and aged rats were subjected to water maze tests at 4 weeks after ICH, as previously described [25]. Animals had to locate a submerged invisible platform located 2 cm below the surface of the water. The platform remained in a fixed location within a round black tub (170 cm diameter) surrounded by fixed extramaze cues. Each animal was given two trials a day for 4 consecutive days, with a maximum of 60 s allowed per trial to locate the platform. Each day, subjects were placed into the tub at a different quadrant location. Each animal was allowed 60 s on the platform after each trial to observe its surroundings. Probe trials were performed by removing the platform on day 5. Each animal was placed into

the quadrant opposite to the target quadrant. The percentage of time the animal spent swimming in the former platform quadrant during a 60 s trial was recorded and used for final analysis (EthoVision; Noldus Information Technology). Swimming speed was calculated to exclude the possibilities of motor impairment effect on maze performance, as suggested by other investigators [26–28].

Biodistribution

MNCs (1×10^7 cells/kg) labeled with Qtracker 655 were administered IV at 24 h after ICH [16]. At 6 and 24 h after MNC injection, animals were sacrificed and perfused with cold PBS followed by 4% PFA. The brain, spleen, liver, lung, and kidney were removed and postfixed in 4% PFA for 24 h and then immersed in 20% sucrose and stored at 4°C for ≥48 h. Twenty micrometer coronal cryosections were then generated and counterstained with 4′,6-diamidino-2-phenylindole (DAPI) for microscopic analysis. Qtracker-positive MNCs were quantified with NIH image software (ImageJ) on three sections of predefined regions of interests (ROIs), involving randomly chosen four fields per section under 200× magnification. The ROIs were in the perihematomal tissue of the brain at the level of sections from +1 to −1 mm relative to the needle insertion point. Random ROIs were also selected from the spleen, liver, lungs, and kidney as described previously [16].

Retired breeder animals

We also examined the effect of MNCs on brain water content, brain atrophy, and cognitive function after ICH in aged animals.

Statistical analysis

Data are presented as the mean ± standard deviation (SD). For hemisphere atrophy and number of stained cells, the Mann–Whitney *U*-test was used for comparison between saline-treated and MNC-treated groups. Analysis of variance (ANOVA) followed by the Tukey–Kramer test was used to compare differences among sham-operated, saline-treated, and MNC-treated groups in brain water content, western blot analysis, and the water maze. For the staircase test, repeated-measures two-way ANOVA and the Bonferroni post-test were used for comparison between saline-treated and MNC-treated groups at different days after ICH. A *P*-value <0.05 was considered statistically significant.

Results

Mortality

Five young and two retired bleeder animals died within 22 h after ICH and were excluded from the experiment. Three young and two retired bleeder animals treated with saline died within 72 h after ICH. There was no mortality after sham-operated or MNC-treated groups in both young and retired bleeder animals.

Immunophenotypes of MNCs

We studied the immunophenotypes of the various cell subpopulations within MNCs. As previously reported in ischemic stroke, MNCs in the rat ICH model are composed of a heterogenous group of different cell types (Table 1).

Table 1. Immuno-Phenotype of MNCs

Cell markers	*Mean*	*SD*
$CD3^+$	6.88	1.29
$CD11b^+$	12.63	1.75
$CD45R^+$	14.57	3.89
$CD161a^+$	1.33	0.25
$CD71^+$	18.55	3.56
$CD34^+$	0.76	0.14
$CD45^-/CD90^+/CD29^+$	0.66	0.11

SD, standard deviation.

MNCs reduced post-ICH inflammation and protected the neurovascular unit

Recent studies indicate that immune modulation may be an important mechanism underlying how certain types of cell therapies, including MNCs, ameliorate brain injury [10,14]. Therefore, we first examined the effect of MNCs on acute inflammation after ICH by using immunohistochemistry ($n = 4$ per group). MPO-positive, iNOS-positive, and OX-42-positive cells were abundant in the perihematomal area, as examined at 3 days after ICH. MNC treatment reduced the number of MPO-positive ($P < 0.05$; Fig. 1A) and iNOS-positive cells ($P < 0.05$; Fig. 1B) compared with those in the saline-treated group. However, there was no significant difference in the number of OX-42-positive cells between MNC and saline treatment groups ($P > 0.05$; Fig. 1C). To further characterize the nature of the injury, we also measured other markers indicative of the neurovascular unit (NVU) responses to ICH by using western blotting ($n = 3$ per group). In the hemorrhagic brain, HMBG1, S100β, MMP9, and AQP4 protein expression was significantly increased compared with sham-operated animals. Treatment with MNCs reduced ICH-mediated HMGB1, S100β, MMP9, and AQP4 expression compared with saline treatment ($P < 0.05$; Fig. 1D). Given that ICH also triggers a systemic immune response, we evaluated two representative inflammatory cytokines in the serum. We found that MNC treatment significantly decreased IL-1β at day 3 after ICH, but did not change IL-10, compared to saline control ($P < 0.05$; Fig. 1F).

MNCs reduced posthemorrhagic cerebral edema and brain atrophy

Since brain edema is one of the most important indices of tissue damage and is frequently linked with inflammation and the loss of blood–brain barrier integrity, we hypothesized that MNCs would reduce cerebral edema. We measured brain water content in adult animals at 3 days after ICH ($n = 6$ per group). Mean brain water content after ICH in the ipsilateral hemisphere was 80.71% ± 0.79% in the saline-treated group and 79.15% ± 0.63% in the MNC-treated group, indicating moderate but significant reduction ($P < 0.05$; Fig. 2A). Since MNCs reduce cerebral edema and posthemorrhagic inflammation, we hypothesized that animals treated with MNCs after ICH would have less neuronal death in perihematomal areas. Using Fluoro-J-stained neurons, MNC treatment significantly reduced neuronal cell death, compared with saline controls ($P < 0.05$; Fig. 1E). We then examined further for tissue protection by examining brain atrophy. At 28 days after ICH, MNC-treated adult

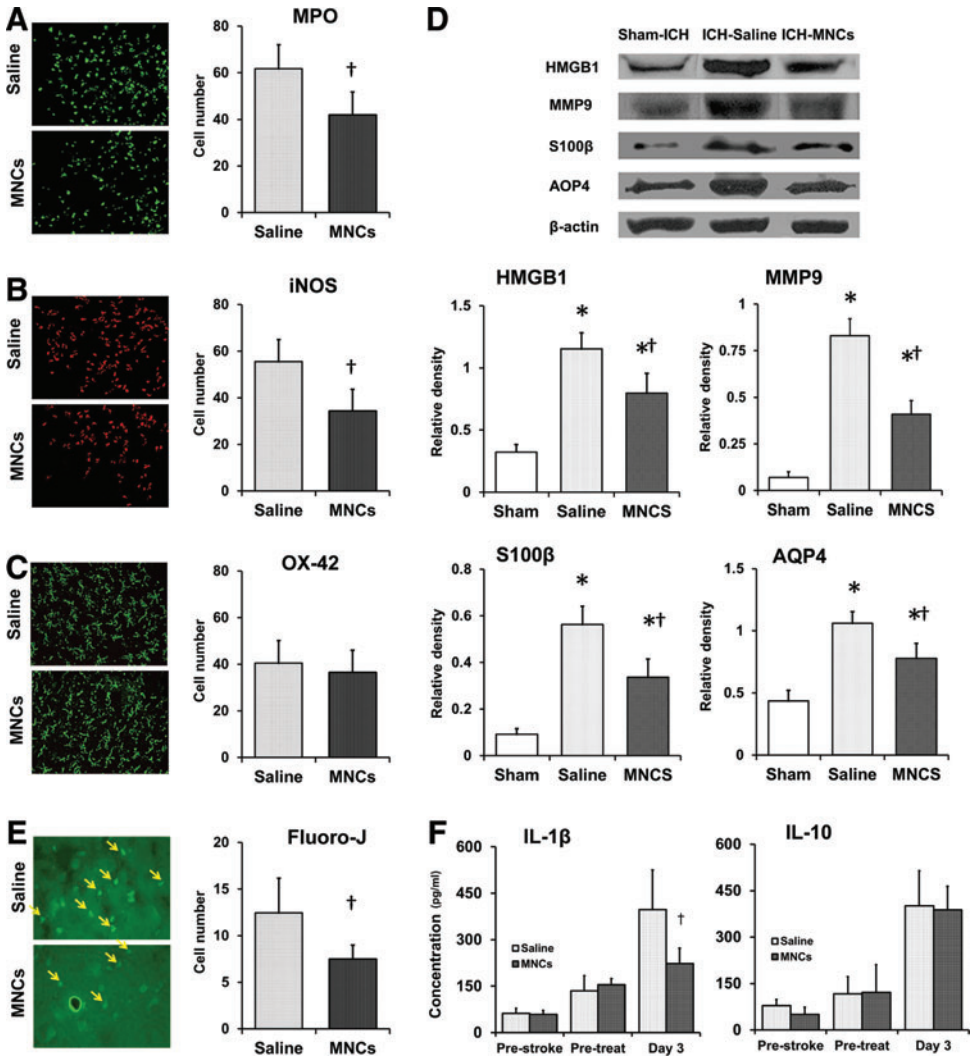

FIG. 1. Mononuclear cells (MNCs) modulate the inflammatory responses in the local brain after intracerebral hemorrhage (ICH). **(A–C)** MNCs lead to modulation of inflammatory cells that have infiltrated into the perihematomal area at day 3 after ICH, compared to saline-treated group: representative fluorescent photomicrographs show **(A)** myeloperoxidase (MPO)-positive cells (*green*), **(B)** inducible nitric oxide synthase (iNOS)-positive cells (*red*), and **(C)** OX-42-positive cells (*green*), and the *right bar* graphs illustrate the quantification analysis of MNC modulation, respectively. Data are the mean ± standard deviation (SD). $^{\dagger}P < 0.05$, compared with saline-treated group after ICH. Magnification: 200×. $n = 4$ per group. **(D)** MNC treatment significantly ameliorated ICH-induced production of high-mobility group protein box-1 (HMGB1), S100 calcium binding protein B (S100β), matrix metalloproteinase-9 (MMP9), and aquaporin (AQP4) protein in the ICH-affected brain. The representative immunoblots and bar graphs show the relative quantitative expression levels of HMGB1, S100β, MMP9, and AQP4 protein in the hemorrhagic hemisphere at day 3 after ICH. Data are the mean ± SD. $^{*}P < 0.05$ compared with sham-ICH-operated group. $^{\dagger}P < 0.05$ compared with saline-treated group after ICH. $n = 3$ per group. **(E)** Representative fluorescent photomicrographs and bar graph show that MNC treatment significantly reduces the Fluoro-J-stained neuron number (*yellow arrows*) in the perihematomal area at day 3 after ICH, compared to saline control. Data are the mean ± SD. $^{\dagger}P < 0.05$, compared with saline-treated group after ICH. Magnification: 630×. $n = 4$ per group. **(F)** Bar graphs indicate that MNC treatment modulates the cytokine level in the serum after ICH. Data are the mean ± SD. $^{\dagger}P < 0.05$, compared with saline-treated group after ICH. $n = 5$ per group. Color images available online at www.liebertpub.com/scd

animals showed significantly less hemispheric atrophy compared with the saline-treated group ($n = 7$ per group; $P < 0.05$; 7.57% ± 1.72% vs. 11.29% ± 3.07%; Fig. 2B).

MNCs enhanced neurogenesis and angiogenesis

Since MNCs are known to stimulate various aspects of repair, we also aimed to investigate neurogenesis, angiogenesis, and functional recovery [29]. First, we assessed DCX-immunohistochemistry in the striatum to detect neuroblasts' migrating toward the hemorrhagic lesion at 28 days after ICH ($n = 4$ per group). MNC treatment increased the presence of DCX-positive cells in the striatum compared with saline treatment ($P < 0.05$; Fig. 3A). Second, we assessed vessel density in the perihematomal area by measuring the number of CD31-labeled vessels at 28 days after ICH ($n = 4$ per group). MNC treatment led to an increase in vessel density compared with saline treatment ($P < 0.05$; Fig. 3B).

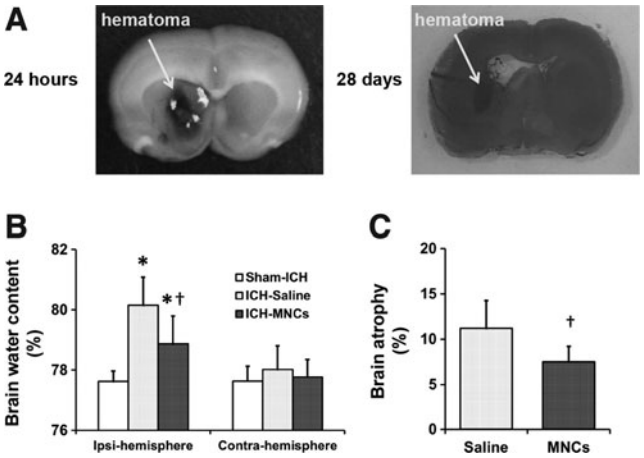

FIG. 2. MNCs reduce perihematomal edema caused by ICH. **(A)** Representative pictures showed the hematomal position at 24 h and 28 days after autologous blood injection (from preliminary data). **(B)** Bar graphs illustrate the brain water content in the hemorrhagic (ipsilateral) and contralateral hemispheres at 3 days after ICH in the sham-, saline-, and MNC-treated ICH groups. Data are the mean ± SD. $^{*}P < 0.05$ compared with the sham-ICH-operated group. $^{\dagger}P < 0.05$ compared with saline-treated group after ICH. $n = 6$ per group. **(C)** Bar graphs illustrate that MNC treatment reduced brain atrophy at day 28 after ICH, compared with the saline-treated group. Data are the mean ± SD. $^{\dagger}P < 0.05$ compared with the saline-treated group. $n = 7$ per group.

MNCs improved motor and cognitive function after ICH

Given that MNCs affect a range of histological endpoints of recovery, we examined the effects of MNCs on long-term motor function ($n = 7$ per group) and spatial learning and memory (sham $n = 13$, saline $n = 12$, MNCs $n = 11$). Young rats treated with MNCs showed significantly greater neurological recovery on the staircase test by 21 or 28 days after ICH ($P < 0.05$; Fig. 4A, B) compared with the saline group. In the water maze, there was no significant difference in swimming speed among the three groups (Fig. 4C). Young rats in the saline-treated group spent significantly less percentage of time in the target quadrant during the 60 s probe trial compared to the sham-operated group ($P < 0.05$; 17.58% ± 8.61% and 30.53% ± 9.28%; Fig. 4D). MNC treatment had a tendency, which was not significant, to improve this cognitive deficit compared with saline treatment ($P = 0.071$; 25.60% ± 6.78% and 17.58% ± 8.61%; Fig. 4D).

Biodistribution

In addition to defining the biological effects of MNCs, we also sought to determine the biodistribution of injected cells [30]. Figure 5 shows representative photomicrographs of the brain, spleen, liver, lung, and kidney sections illustrating fluorescence-labeled MNCs 6 and 24 h after IV administration ($n = 4$ per time point). Among Qtracker-labeled MNCs that entered the brain, we estimate over 90% migrated in the perihematomal area as early as 6 h after IV

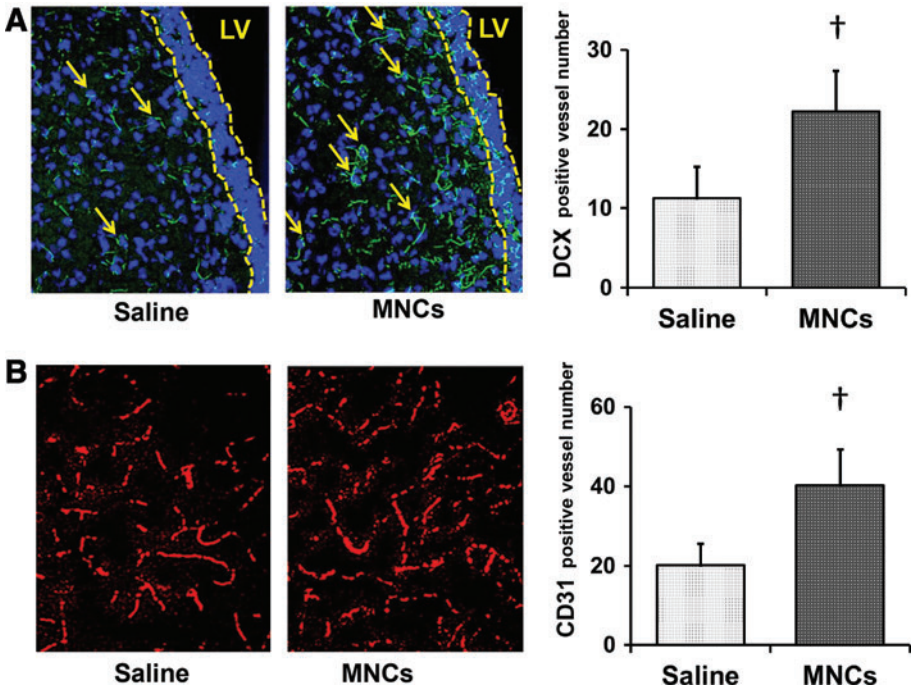

FIG. 3. MNCs improved neurogenesis and angiogenesis at day 28 after ICH. **(A)** The representative photomicrographs showing the neuroblasts in the striatum near the subventricular zone. Only cells with the double doublecortin (DCX; *green*) and nuclear marker 4′,6-diamidino-2-phenylindole (DAPI) staining were enumerated as DCX-positive cells (*arrows*). The subventricular zone is shown as the area between the two broken *yellow lines*. Bar graph on the *right* shows the number of DCX-positive cells in the striatum in saline- and MNC-treated rats. $^{\dagger}P < 0.05$, compared with the saline-treated group. Magnification: 200×. $n = 4$ per group. **(B)** Representative photomicrographs showing CD31-labeled blood vessels (*red*) at day 28 after stroke. Bar graphs on the *right* show the vessel numbers in saline- and MNC-treated rats. $^{\dagger}P < 0.05$, compared with saline-treated group. Magnification: 200×. $n = 4$ per group. LV, lateral ventricle. Color images available online at www.liebertpub.com/scd

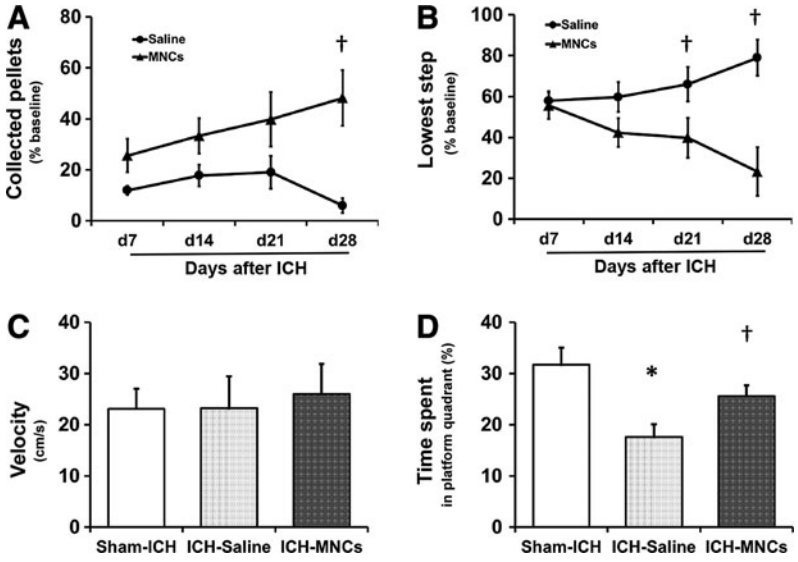

FIG. 4. MNCs improved sensorimotor functional recovery after ICH. Sensorimotor function was evaluated by the staircase test: line diagrams indicate the alternation of the collected pellets on the *right* staircase **(A)** and the lowest step reached **(B)** in the staircase test over time from day 7 to 28 after ICH in rats after ICH treated with saline (control) or MNC. Data are the mean ± SD. $^{\dagger}P < 0.05$, compared with the saline-treated group. $n = 7$ per group. Cognitive dysfunction at 4 weeks after ICH in sham group and in animals after ICH treated with saline or MNC was evaluated by the Morris water maze test using the percent time spent in the platform quadrant during the probe trial. The swimming speed was the same for all the groups **(C)**. The bar graph shows time spent in the target quadrant by sham rats and rats after ICH treated with saline (control) or MNC. **(D)**. Data are the mean ± SD. $^{*}P < 0.05$ compared with sham-ICH-operated group. $^{\dagger}P = 0.071$, compared with saline-treated group. Sham $n = 13$, saline $n = 12$, and MNCs $n = 11$.

infusion. MNCs were also observed in the spleen, liver, lung, and kidney. There was a significant decrease in the number of labeled MNCs over time at the 24 h time point.

Retired breeder animals

Since ICH affects the elderly population, we sought to establish whether MNCs may also benefit aged rats. MNC treatment after ICH (applied in the same manner as young rats) reduced brain water content at 3 days ($n = 6$ per group; $P < 0.05$; 80.15% ± 0.93% vs. 78.86% ± 0.93%; Fig. 6A) and brain atrophy at 28 days ($n = 7$ per group; $P < 0.05$; 9.08% ± 3.10% vs. 12.72 ± 2.78; Fig. 6B) compared with the saline-treated group. The staircase test was not performed on aged rats because of size and performance limitations. Based on our experience from preliminary experiments, aged animals will not meet training requirements to perform modality-specific tasks as complex as reaching tasks. Aged animals in the saline-treated group spent significantly less percentage of time in the water maze target quadrant

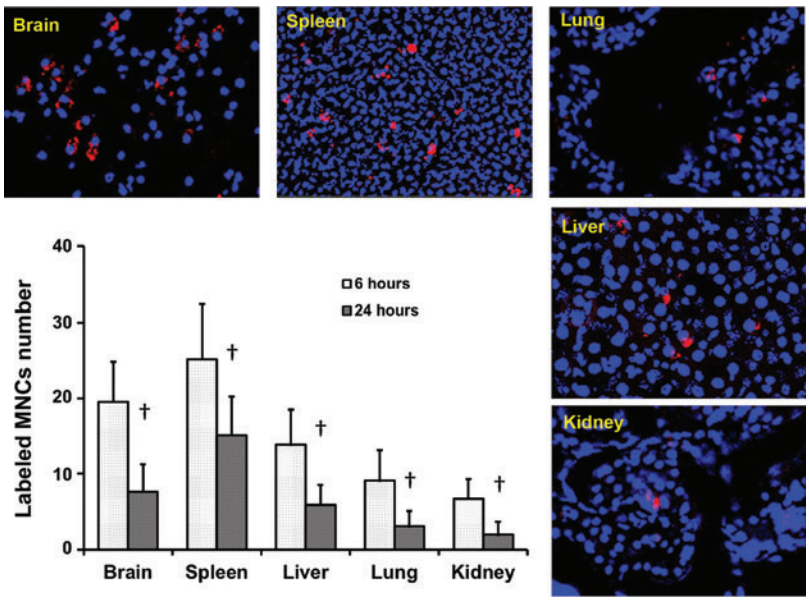

FIG. 5. MNC biodistributions at 6 and 24 h after IV administration in the ICH model. The representative fluorescence images and bar graph show the number of the Qtracker-labeled MNCs (*red*) in the brain, spleen, lungs, liver, and kidney. *Red*: Qtracker 655; *blue*: DAPI. Magnification: 200×. The y-axis is the mean number of cells collected from each section. Data are the mean ± SD. $^{\dagger}P < 0.05$, compared with 6 h, $n = 4$ per time point. Color images available online at www.liebertpub.com/scd

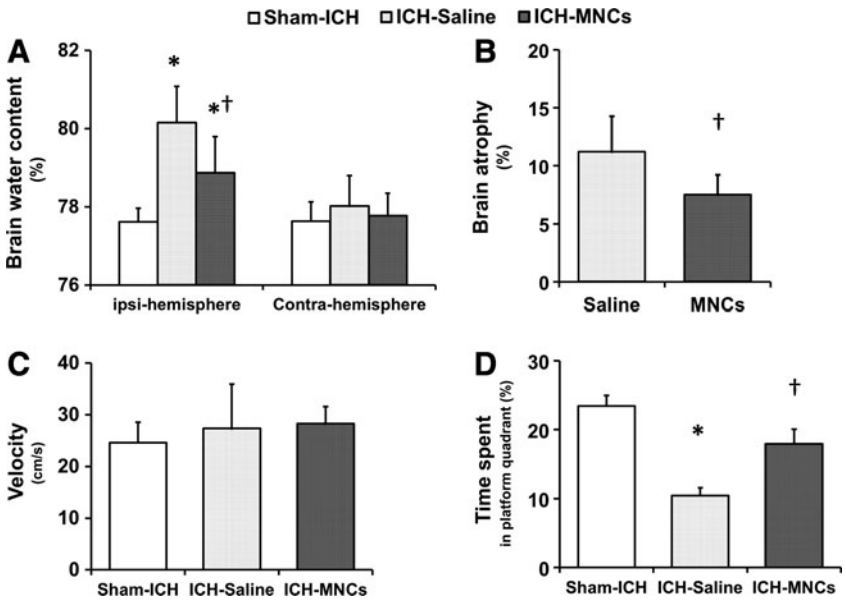

FIG. 6. The effect of MNCs on ICH outcome in retired bleeder Long Evans rat. **(A)** Bar graph illustrating the brain water content in the hemorrhagic (ipsilateral) and contralateral hemispheres. Data are the mean ± SD. $^{*}P < 0.05$ compared with the sham-ICH-operated group. $^{\dagger}P < 0.05$ compared with saline-treated group. $n = 6$ per group. **(B)** Bar graph illustrating that MNC reduced brain atrophy in animals at day 28 after ICH, compared with saline-treated controls. Data are the mean ± SD. $^{\dagger}P < 0.05$ compared with saline-treated group. $n = 7$ per group. **(C, D)** The outcomes of Morris water maze test performed at 4 weeks after ICH. Bar graphs illustrate swimming speed **(C)** and the time spent in the target quadrant **(D)** in the sham-ICH group and ICH groups treated with saline or MNC. Data are the mean ± SD. $^{*}P < 0.05$ compared with sham-ICH-operated group. $^{\dagger}P < 0.05$ compared with saline-treated group. Sham $n = 13$, saline $n = 12$, and MNCs $n = 10$.

compared to the sham-operated group (sham $n = 13$, saline $n = 12$, MNCs $n = 10$; $P < 0.05$; 17.39% ± 6.57% and 39.01% ± 9.38%; Fig. 6D), as assessed at 4 weeks after ICH. The time MNC-treated rats swam in the target quadrant was significantly more than the saline-treated group ($P < 0.05$; 29.88% ± 11.95% and 17.39% ± 6.57%; Fig. 6D). There was no significant difference in the swimming speed among the groups (Fig. 6C).

Discussion

Cell-based therapy has been proposed as a potential treatment for various neurological disorders. Bone marrow-derived MNCs are a promising potential therapy for acute neurological disorders such as stroke and traumatic brain injury because they can be rapidly isolated and reinfused for autologous applications without the need for cell culture [8]. MNCs are a heterogeneous population of cells that include mesenchymal stem cells, hematopoietic progenitor cells, endothelial progenitor cells, and several different committed cells of various lineages. Previous reports have demonstrated that MNCs conferred beneficial effects against various types of brain damage, including models of focal cerebral ischemia, transient global cerebral ischemia, chronic cerebral ischemia, and traumatic brain injury [9,31–33]. In this study, we now show that intravenous administration of autologous MNCs reduces injury and enhances recovery in the autologous blood injection ICH model. We administered the cells at 24 h after injury because our studies on ischemic stroke suggest that the inflammatory response may be an important target of MNCs and the time window appears to be a clinically practical time point to harvest bone marrow from stroke patients [14].

Because ICH is known to cause robust inflammation [34] with neutrophil infiltration [35] and MNCs are recognized to reduce proinflammatory signals in ischemic stroke, we first assessed the impact of MNCs on inflammation in ICH. We found that MNCs reduce the number of neutrophils in the perihematomal area at 3 days after injury. There was no significant difference in the number of microglia/macrophages between MNC or saline treatment groups. Interestingly, the total numbers of iNOS-positive cells were significantly lower in the perihematomal area in the MNC-treated group. Furthermore, the levels of serum IL-1β were decreased at day 3 after ICH by MNC treatment, which supports the recent report that the administration of MNCs suppresses various proinflammatory cytokines such as IL-1β and IL-6 [36]. These results support the hypothesis that MNCs reduce proinflammatory responses both within the central nervous system and in the periphery.

Inflammation after ICH is tightly linked with cerebral edema, disruption of the NVU, and secondary neuronal injury. We therefore assessed brain water content at 3 days after ICH, a time point when edema is known to peak [37,38]. We found a modest but significant reduction of brain water content in the MNC-treated group compared with the saline-treated group. These results suggest that MNCs could ameliorate brain edema, even when treatment is delayed by 24 h. There have been other reports that cell therapies can reduce cerebral edema following brain injury [10,39]. To explore potential mechanisms, we investigated AQP4, a major brain water channel, which is primarily expressed in perimicrovessel astrocyte foot processes and is implicated in cerebral edema formation and resolution [40]. We found that MNCs reduced the expression of AQP4 in perihematomal areas, which is in concert with another study in which mesenchymal stem cells were found to reduce brain edema by inhibiting AQP4 upregulation in astrocytes after cerebral ischemia [41].

We further found that MNCs reduce the expression of other proteins related to inflammation in ICH, including MMP9, HMBG1, and S100B, all of which are directly or indirectly related to disruption of the NVU. MMP9 is activated by brain injury, which may lead to collapse of the NVU and detachment of astrocyte end feet from the basal lamina [42]. Perihematomal edema is also closely associated with MMP9 levels and neurological worsening. We found that MNC treatment leads to the reduction of other inflammatory

mediators. For example, HMGB1, high-mobility group protein 1, is a protein from the group of alarmins, which is released by damaged brain cells and activated immune cells. Upon release, HMGB1 acts as an early proinflammatory cytokine within the NVU, which leads to exacerbation of proinflammatory responses, and blood-brain barrier breakdown in the ICH model [43,44]. S100B is released by activated astrocytes and is associated with enhanced reactive gliosis and further exacerbation of brain injury [45]. Increased S100B levels are also found after acute spontaneous ICH in patients, in association with acute worsening [46]. Although the roles of these selected proteins in the pathology of ICH are not entirely clear, our findings suggest that MNCs may target and prevent various active proinflammatory processes that are linked to secondary injury in the acute stages of ICH. To further corroborate that MNCs confer neurovascular protection, we also found that MNCs administered at 24 h after ICH reduced neuronal cell death in perihematomal areas and brain atrophy compared with saline control.

Many types of cell therapies do not solely target one pathologic process in acute neurological injury models. MNCs, in particular, not only modulate inflammatory and immune-mediated responses but also upregulate various aspects of repair in rodents with ischemic stroke. One aspect of brain repair may be the migration of neuroblasts toward the damaged area, which has been shown to occur in the blood injection rat ICH model and possibly in the brains of patients after ICH [47]. There may be some concordance between neurogenesis and functional improvement after brain injury [48]. In our present study, there was a significant increase in number of DCX-positive neuroblasts in MNC-treated animals compared with saline treatment at 28 days after ICH. The regenerated neuroblasts may produce factors that improve tissue integrity of the damaged brain [49]. We also examined the effect of MNCs on vessel density. Several studies have shown that MNCs provide protection in a model of chronic cerebral ischemia-induced cognitive dysfunction by increasing angiogenesis [50,51]. Others have demonstrated that MNCs increase vascular density and blood flow in various ischemic disorders such as cardiovascular disease, peripheral arterial disease, and diabetic foot [52]. We also found a significant increase in the number of vessels in the perihematomal area in MNC-treated animals. Thus, our study overall suggests that MNCs may increase two important aspects of brain repair in addition to modulating the inflammatory response after ICH. However, it is important to point out that MNCs may be exerting a protective effect on immature neurons and CD31-positive endothelial cells and that more studies would be needed to prove more definitively that MNCs increase angiogenesis and neurogenesis.

To therapeutically characterize the effects of MNCs after ICH, we also assessed the long-term functional outcome. Based on the STAIR recommendations, we examined motor and cognitive functions [53]. We found significantly greater motor recovery on the staircase test in animals treated with MNCs. Furthermore, we observed a tendency toward improvement in spatial learning in MNC-treated animals compared with saline controls.

Finally, we performed a biodistribution study to monitor the migration and fate of injected cells. Labeled MNCs delivered by intravenous administration were observed in perihematomal areas as early as 6 h after IV injection. However, we also found a greater number of MNCs in the spleen and also detected labeled cells in the liver, lung, and kidney. Consistent with other studies, MNCs substantially decrease in numbers within 24 h of injection [16,17,54,55]. These findings are in line with prior studies that MNCs likely selectively migrate to injured areas in the brain [15] and that the injected cells migrate more to other peripheral organs that may reflect the upregulation of the peripheral immune response to brain injury. Based on our prior studies, the reduction in labeled MNCs likely indicates that the MNCs are dying over time [16]. However, we did not determine the different populations of MNCs that migrated to the perihematomal area. Another important issue is that differences in labeling techniques (eg, Qtracker vs. GFP) might lead to different biodistribution results [56,57].

The STAIR guidelines also recommend additional studies in older animals [55]. We therefore repeated some selective studies using retired bleeder rats. As seen in young rats, MNCs in this model reduced brain edema and brain atrophy and improved spatial learning and memory produced by ICH. Although we did not repeat the neurogenesis and angiogenesis experiments on aged rats in the present study, recent studies provide evidence that recovery of motor and spatial memory impairment by cellular therapy was associated with the improvement of neurogenesis and angiogenesis, even in aged rats after stroke [57,58].

In conclusion, MNC treatment, in a clinically relevant manner, appears to have therapeutic effects on ICH by reducing edema and inflammatory processes in the acute phase and enhancing endogenous restorative responses in the chronic phase. These effects might underlie improved long-term behavioral recovery. A recent clinical study suggests that autologous intracerebral MNC implantation may improve neurological outcome in patients with ICH [59]. Because MNCs are a mixture of different cell types, further studies will be needed to determine which cell populations may be responsible for their beneficial effects and which cell subpopulations of the injected MNCs are in the brain. Further studies will also be needed to better dissect whether MNCs act at the local regional level within the brain or more directly on the systemic and peripheral immune responses after ICH. Nevertheless, the data from this study lead us to speculate that MNCs may have the potential to exert broad short- and long-term effects after ICH. Further studies are also needed to determine the therapeutic time window; testing in animals with comorbid conditions should also be considered for clinical application.

Acknowledgments

This research work was supported, in part, by grants from the National Institutes of Health R21 NS064316 and R-01 NS071127. All experiments were conducted in compliance with the ARRIVE guidelines.

Author Disclosure Statement

No competing financial interests exist.

References

1. Broderick J, S Connolly, E Feldmann, D Hanley, C Kase, et al. (2007). Guidelines for the management of spontaneous intracerebral hemorrhage in adults: 2007 update: a guideline from the American Heart Association/American

Stroke Association Stroke Council, High Blood Pressure Research Council, and the Quality of Care and Outcomes in Research Interdisciplinary Working Group. Stroke 38:2001–2023.
2. Jorgensen HS, H Nakayama, HO Raaschou and TS Olsen. (1995). Intracerebral hemorrhage versus infarction: stroke severity, risk factors, and prognosis. Ann Neurol 38:45–50.
3. Morgenstern LB, JC Hemphill 3rd, C Anderson, K Becker, JP Broderick, et al. (2010). Guidelines for the management of spontaneous intracerebral hemorrhage: a guideline for healthcare professionals from the American Heart Association/American Stroke Association. Stroke 41:2108–2129.
4. Abe K, T Yamashita, S Takizawa, S Kuroda, H Kinouchi, et al. (2012). Stem cell therapy for cerebral ischemia: from basic science to clinical applications. J Cereb Blood Flow Metab 32:1317–1331.
5. Saito H, K Magota, S Zhao, N Kubo, Y Kuge, et al. (2013) 123I-iomazenil single photon emission computed tomography visualizes recovery of neuronal integrity by bone marrow stromal cell therapy in rat infarct brain. Stroke 44:2869–2874.
6. Taguchi A, T Soma, H Tanaka, T Kanda, H Nishimura, et al. (2004). Administration of CD34+ cells after stroke enhances neurogenesis via angiogenesis in a mouse model. J Clin Invest 114:330–338.
7. Andres RH, N Horie, W Slikker, H Keren-Gill, K Zhan, et al. (2011). Human neural stem cells enhance structural plasticity and axonal transport in the ischaemic brain. Brain 134:1777–1789.
8. Savitz SI, V Misra, M Kasam, H Juneja, CS Cox, Jr., et al. (2011). Intravenous autologous bone marrow mononuclear cells for ischemic stroke. Ann Neurol 70:59–69.
9. Iihoshi S, O Honmou, K Houkin, K Hashi and JD Kocsis. (2004). A therapeutic window for intravenous administration of autologous bone marrow after cerebral ischemia in adult rats. Brain Res 1007:1–9.
10. Lee ST, K Chu, KH Jung, SJ Kim, DH Kim, et al. (2008). Anti-inflammatory mechanism of intravascular neural stem cell transplantation in haemorrhagic stroke. Brain 131:616–629.
11. Otero L, M Zurita, C Bonilla, C Aguayo, A Vela, et al. (2011). Late transplantation of allogeneic bone marrow stromal cells improves neurologic deficits subsequent to intracerebral hemorrhage. Cytotherapy 13:562–571.
12. Karki K, RA Knight, Y Han, D Yang, J Zhang, et al. (2009). Simvastatin and atorvastatin improve neurological outcome after experimental intracerebral hemorrhage. Stroke 40:3384–3389.
13. Felberg RA, JC Grotta, AL Shirzadi, R Strong, P Narayana, et al. (2002). Cell death in experimental intracerebral hemorrhage: the black hole model of hemorrhagic damage. Ann Neurol 51:517–524.
14. Yang B, X Xi, J Aronowski and SI Savitz. (2012). Ischemic stroke may activate bone marrow mononuclear cells to enhance recovery after stroke. Stem Cells Dev 21:3332–3340.
15. Brenneman M, S Sharma, M Harting, R Strong, CS Cox, Jr., et al. (2010). Autologous bone marrow mononuclear cells enhance recovery after acute ischemic stroke in young and middle-aged rats. J Cereb Blood Flow Metab 30:140–149.
16. Yang B, R Strong, S Sharma, M Brenneman, K Mallikarjunarao, et al. (2011). Therapeutic time window and dose response of autologous bone marrow mononuclear cells for ischemic stroke. J Neurosci Res 89:833–839.
17. Yang B, E Migliati, K Parsha, K Schaar, X Xi, et al. (2013). Intra-arterial delivery is not superior to intravenous delivery of autologous bone marrow mononuclear cells in acute ischemic stroke. Stroke 44:3463–3472.
18. Jung KH, K Chu, SW Jeong, SY Han, ST Lee, et al. (2004). HMG-CoA reductase inhibitor, atorvastatin, promotes sensorimotor recovery, suppressing acute inflammatory reaction after experimental intracerebral hemorrhage. Stroke 35:1744–1749.
19. Keep RF, Y Hua and G Xi. (2012). Brain water content. A misunderstood measurement? Transl Stroke Res 3:263–265.
20. Montoya CP, LJ Campbell-Hope, KD Pemberton and SB Dunnett. (1991). The staircase test: a measure of independent forelimb reaching and grasping abilities in rats. J Neurosci Methods 36:219–228.
21. Schaar KL, MM Brenneman and SI Savitz. (2010). Functional assessments in the rodent stroke model. Exp Transl Stroke Med 2:13.
22. Bouet V, T Freret, J Toutain, D Divoux, M Boulouard, et al. (2007). Sensorimotor and cognitive deficits after transient middle cerebral artery occlusion in the mouse. Exp Neurol 203:555–567.
23. MacLellan CL, AM Auriat, SC McGie, RH Yan, HD Huynh, et al. (2006). Gauging recovery after hemorrhagic stroke in rats: implications for cytoprotection studies. J Cereb Blood Flow Metab 26:1031–1042.
24. MacLellan CL, LM Davies, MS Fingas and F Colbourne. (2006). The influence of hypothermia on outcome after intracerebral hemorrhage in rats. Stroke 37:1266–1270.
25. Morris RG, P Garrud, JN Rawlins and J O'Keefe. (1982). Place navigation impaired in rats with hippocampal lesions. Nature 297:681–683.
26. Thompson HJ, DG LeBold, N Marklund, DM Morales, AP Hagner, et al. (2006). Cognitive evaluation of traumatically brain-injured rats using serial testing in the Morris water maze. Restor Neurol Neurosci 24:109–114.
27. Jolkkonen J, NP Gallagher, K Zilles and J Sivenius. (2003). Behavioral deficits and recovery following transient focal cerebral ischemia in rats: glutamatergic and GABAergic receptor densities. Behav Brain Res 138: 187–200.
28. Ortega FJ, J Jolkkonen, N Mahy and MJ Rodriguez. (2013). Glibenclamide enhances neurogenesis and improves long-term functional recovery after transient focal cerebral ischemia. J Cereb Blood Flow Metab 33:356–364.
29. Masuda T, Y Isobe, N Aihara, F Furuyama, S Misumi, et al. (2007). Increase in neurogenesis and neuroblast migration after a small intracerebral hemorrhage in rats. Neurosci Lett 425:114–119.
30. Savitz SI, M Chopp, R Deans, T Carmichael, D Phinney, et al. (2011). Stem cell therapy as an emerging paradigm for stroke (STEPS) II. Stroke 42:825–829.
31. Bedi SS, PA Walker, SK Shah, F Jimenez, CP Thomas, et al. (2013). Autologous bone marrow mononuclear cells therapy attenuates activated microglial/macrophage response and improves spatial learning after traumatic brain injury. J Trauma Acute Care Surg 75:410–416.
32. Maruichi K, S Kuroda, Y Chiba, M Hokari, H Shichinohe, et al. (2009). Transplanted bone marrow stromal cells improves cognitive dysfunction due to diffuse axonal injury in rats. Neuropathology 29:422–432.
33. Ramos AB, A Vasconcelos-Dos-Santos, SA Lopes de Souza, PH Rosado-de-Castro, LM Barbosa da Fonseca,

et al. (2013). Bone-marrow mononuclear cells reduce neurodegeneration in hippocampal CA1 layer after transient global ischemia in rats. Brain Res 1522:1–11.
34. Aronowski J and CE Hall. (2005). New horizons for primary intracerebral hemorrhage treatment: experience from preclinical studies. Neurol Res 27:268–279.
35. Zhao XSG, H Zhang, S-M Ting, S Song, N Gonzales and J Aronowski. (2014). Polymorphonuclear neutrophil in brain parenchyma after experimental intracerebral hemorrhage. Transl Stroke Res 5:554–561.
36. Leal MM, ZS Costa-Ferro, BS Souza, CM Azevedo, TM Carvalho, CM Kaneto, et al. (2014). Early transplantation of bone marrow mononuclear cells promotes neuroprotection and modulation of inflammation after status epilepticus in mice by paracrine mechanisms. Neurochem Res 39:259–268.
37. Xi G, RF Keep and JT Hoff. (2006). Mechanisms of brain injury after intracerebral haemorrhage. Lancet Neurol 5:53–63.
38. Hua Y, T Schallert, RF Keep, J Wu, JT Hoff, et al. (2002). Behavioral tests after intracerebral hemorrhage in the rat. Stroke 33:2478–2484.
39. Borlongan CV, JG Lind, O Dillon-Carter, G Yu, M Hadman, et al. (2004). Bone marrow grafts restore cerebral blood flow and blood brain barrier in stroke rats. Brain Res 1010:108–116.
40. Badaut J, F Lasbennes, PJ Magistretti and L Regli. (2002). Aquaporins in brain: distribution, physiology, and pathophysiology. J Cereb Blood Flow Metab 22:367–378.
41. Tang G, Y Liu, Z Zhang, Y Lu, Y Wang, et al. (2014). Mesenchymal stem cells maintain blood-brain barrier integrity by inhibiting aquaporin-4 up-regulation after cerebral ischemia. Stem Cells 32:3150–3162.
42. Yamashita T, T Kamiya, K Deguchi, T Inaba, H Zhang, et al. (2009). Dissociation and protection of the neurovascular unit after thrombolysis and reperfusion in ischemic rat brain. J Cereb Blood Flow Metab 29:715–725.
43. Ohnishi M, H Katsuki, C Fukutomi, M Takahashi, M Motomura, et al. (2011). HMGB1 inhibitor glycyrrhizin attenuates intracerebral hemorrhage-induced injury in rats. Neuropharmacology 61:975–980.
44. Hayakawa K, J Qiu and EH Lo. (2010). Biphasic actions of HMGB1 signaling in inflammation and recovery after stroke. Ann N Y Acad Sci 1207:50–57.
45. Mori T, J Tan, GW Arendash, N Koyama, Y Nojima, et al. (2008). Overexpression of human S100B exacerbates brain damage and periinfarct gliosis after permanent focal ischemia. Stroke 39:2114–2121.
46. Delgado P, J Alvarez Sabin, E Santamarina, CA Molina, M Quintana, et al. (2006). Plasma S100B level after acute spontaneous intracerebral hemorrhage. Stroke 37:2837–2839.
47. Shen J, L Xie, X Mao, Y Zhou, R Zhan, et al. (2008). Neurogenesis after primary intracerebral hemorrhage in adult human brain. J Cereb Blood Flow Metab 28:1460–1468.
48. Wiltrout C, B Lang, Y Yan, RJ Dempsey and R Vemuganti. (2007). Repairing brain after stroke: a review on post-ischemic neurogenesis. Neurochem Int 50:1028–1041.
49. Shen LH, Y Li and M Chopp. (2010). Astrocytic endogenous glial cell derived neurotrophic factor production is enhanced by bone marrow stromal cell transplantation in the ischemic boundary zone after stroke in adult rats. Glia 58:1074–1081.
50. Fujita Y, M Ihara, T Ushiki, H Hirai, S Kizaka-Kondoh, et al. (2010). Early protective effect of bone marrow mononuclear cells against ischemic white matter damage through augmentation of cerebral blood flow. Stroke 41:2938–2943.
51. Wang J, X Fu, C Jiang, L Yu, M Wang, et al. (2014). Bone marrow mononuclear cell transplantation promotes therapeutic angiogenesis via upregulation of the VEGF-VEGFR2 signaling pathway in a rat model of vascular dementia. Behav Brain Res 265:171–180.
52. Raval Z and DW Losordo. (2013). Cell therapy of peripheral arterial disease: from experimental findings to clinical trials. Circ Res 112:1288–1302.
53. Stroke Therapy Academic Industry Roundtable (STAIR). (1999) Recommendations for standards regarding preclinical neuroprotective and restorative drug development. Stroke 30:2752–2758.
54. Kamiya N, M Ueda, H Igarashi, Y Nishiyama, S Suda, et al. (2008). Intra-arterial transplantation of bone marrow mononuclear cells immediately after reperfusion decreases brain injury after focal ischemia in rats. Life Sci 83:433–437.
55. Fisher M, G Feuerstein, DW Howells, PD Hurn, TA Kent, et al. (2009). Update of the stroke therapy academic industry roundtable preclinical recommendations. Stroke 40:2244–2250.
56. Nakano-Doi A, T Nakagomi, M Fujikawa, N Nakagomi, S Kubo, S Lu, et al. (2010). Bone marrow mononuclear cells promote proliferation of endogenous neural stem cells through vascular niches after cerebral infarction. Stem Cells 28:1292–1302.
57. Balseanu AT, AM Buga, B Catalin, DC Wagner, J Boltze, et al. (2014). Multimodal approaches for regenerative stroke therapies: combination of granulocyte colony-stimulating factor with bone marrow mesenchymal stem cells is not superior to G-CSF alone. Front Aging Neurosci 6:130.
58. Popa-Wagner A, AM Buga, TR Doeppner and DM Hermann. (2014). Stem cell therapies in preclinical models of stroke associated with aging. Front Cell Neurosci 8:347.
59. Li ZM, ZT Zhang, CJ Guo, FY Geng, F Qiang and LX Wang. (2013). Autologous bone marrow mononuclear cell implantation for intracerebral hemorrhage-a prospective clinical observation. Clin Neurol Neurosurg 115:72–76.

Address correspondence to:
Dr. Bing Yang
Department of Neurology
University of Texas Medical School at Houston
MSB 7.617
6431 Fannin Street
Houston, TX 77030

E-mail: bing.yang@uth.tmc.edu

Received for publication March 25, 2015
Accepted after revision September 18, 2015
Prepublished on Liebert Instant Online September 28, 2015